A new hybrid method for H_2S-sensitive devices using WO_3-based film and ACF interconnect

2013 Meas. Sci. Technol. 24 075105

(http://iopscience.iop.org/0957-0233/24/7/075105)

Meas. Sci. Technol. **24** (2013) 075105 (7pp) doi:10.1088/0957-0233/24/7/075105

A new hybrid method for H_2S-sensitive devices using WO_3-based film and ACF interconnect

Li Min Kuo[1,3], **Yu-Tai Shih**[2], **Cen-Shawn Wu**[2], **Yu-Chi Lin**[1] **and Shuchi Chao**[1]

[1] Department of Electrophysics, National Chiao Tung University, Science Building III, 1001 University Road, Hsinchu, 300, Taiwan
[2] Department of Physics, National Changhua University of Education, No.1 Jin De Road, Changhua 500, Taiwan
[3] Department of Surgery, Medicine School, Stanford University, CA 95305, USA

E-mail: lmkuo@ieee.org

Received 10 December 2012, in final form 16 May 2013
Published 17 June 2013
Online at stacks.iop.org/MST/24/075105

Abstract
A new hybrid integration method has been reported for process simplification of conventional metal-oxide sensors with a gold (Au) dopant-like catalyst during hydrogen sulfide (H_2S) gas detections at room temperature. Different from conventional fabrications, an anisotropic conduction film (ACF) followed by a sputtered tungsten oxide (WO_3) film tapped on Cu electrodes has been utilized in consumer applications. The process steps were reduced without compromising electrical performances. The treated ACF with a thin WO_3 film, coated across two closely spaced microelectrodes is employed as the H_2S solid-state sensor at room temperature. Apart from exhibiting good interconnects as conductive bumps, Au dopant-like catalyst within ACF will also produce a lower barrier between the bands of electronics, and therefore improve the electrical conductivity significantly. Our integration method offers a number of merits, including high sensitivity to the reference gas, lead-free bonding connection, low-temperature fabrication, high throughput and less fabrication time.

Keywords: H_2S, gas sensor, ACF, WO_3, Au-catalyst

(Some figures may appear in colour only in the online journal)

1. Introduction

In present times, social consciousness about quality, food safety and environmental protection has been raised significantly [1]. The presence of colorless, toxic and flammable gas such as hydrogen sulfide (H_2S) is hazardous in our daily life [2]. From the viewpoint of health concern, H_2S gas is an irritant and a chemical asphyxiate with effects on both oxygen utilization and the central nervous system [3, 4]. Based on chemical reduction and oxidation reactions taking place on the sensor surface, solid-state elements for gas detection have received much attention in many works [5–9]. Tungsten oxide (WO_3) used for the production of tungsten metal powder or as compound and pigment for ceramics has been investigated, in particular for the application of surface acoustic wave (SAW) devices as a highly sensitive sensor for H_2S gas in ambient air [10, 11]. With good thermal stability, WO_3 device with Pt-dopant catalyst has been considered effective for H_2S gas detection, since the metal acted as a good dopant for the detection of H_2S gas in air [12]. Tao *et al* utilized platinum (Pt), gold (Au) or Au–Pt noble metals deposited over WO_3 film as an activator layer using a sputtering approach and reported good sensitivity up to 220 °C [13]. Xu *et al* also demonstrated the electrical properties of both intrinsic and Au-doped WO_3 film prepared by an RF (radio-frequency) sputtering technique [14]. However, more sophisticated process flows as well as bulky metal-doping equipment on the components should be investigated to improve the sensitivity during the operation

of gas detections. In consideration of designing a simplified solid-state device, which can detect the precise concentration of the single component toxic gas immediately, a more straightforward fabrication process will be investigated as necessary for compact and portable H_2S gas monitors.

In this work, a hybrid integration process has been developed for the simplification of the fabrication process that consists of a WO_3-based gas sensor and an anisotropic conduction tape-bonding technique. Anisotropic conductive film (ACF), a lead-free epoxy material employed in our experiments, achieved more compact assembling without soldering [15–18]. Additionally, at room temperature, Au particles similar to conductive bumps not only provide the electrical interconnection through ACF to electrodes but also offer some advantages such as producing enhanced compression, improving thermal conduction, maintaining space between chips, preventing a short circuit through the substrate, and acting as a mechanical stress reliever in the flip chip assembly [19]. As a result of the catalysis, contributed from Au particles distributed uniformly inside ACF, after exposure to reference gas, a significant reduction on the WO_3-based sensor occurs that generates conductometric change. No bulky equipment or other support is necessary for doping the metal on the components. The proposed chemical-sensitive device is useful as the basis of construction of durable microsensors for tracing the concentration gradient in food freshness and safety detection toward consumer applications operating at room temperature.

2. Experimental details

2.1. Sensor fabrication

A pair of adjacent Cu-pad electrodes was well defined on PCB (printed circuit board) by lithography technique. The Cu electrodes, separated by a distance of 237 μm, were typically 735 μm in width and 1400 μm in length (excluding the lead portion with the diameter of 400 μm). Before use, the Cu-electrode surface was further treated in sequence with de-ionized water, trichloroethane, acetone and de-ionized water by vibration in an ultrasonic cleaner. Then, the chip was purged with a dry N_2 jet, followed by a dehydration bake at 120 °C for 30 min.

ACF (CP8830IH4; 2.35 $\times$ 10^8 mm^{-3} surface density, 52 ppm/°C heat-inflation coefficient and 1.8% rate of humidity absorption; SONY Chemicals Inc.) without the cover film was used to tap on the Cu-electrode surface, followed by the pre-bonding process applied to the device with a 5 kgf (kilogram force) suppression at 80 °C for 5 s. After the strength of the post-suppression (15 kgf) was applied at 185 °C for 15 s, the base film (PET film) was removed, followed by a WO_3-sputtered film deposition. The adhesion between Au particles inside the ACF and Cu electrodes was improved, and dehydration of the ACF was also achieved due to the high-temperature treatment. In addition, the Au particles will be revealed due to the shrinkage in thickness of the resin within the ACF.

The prepared WO_3 (3000 Å thickness, 4.77 g cm^{-3} density and 99.99% purity, Pure Tech Inc.) was robust and adhered strongly to the ACF/Cu-pad surface by the magnetron RF-sputtering technique at 110 W. With the same apparatus as used before [20, 21], the WO_3 film application was carried out under 50% O_2 in argon at a total pressure of 70 mTorr in a magnetron sputtering source (A-320 AJA) powered by an RF generator (PFG-600 F Hutinger) with a matchbox (PFM-750). No difficulty, such as peeling or swelling by hydration, was encountered throughout the course of our experiments. After the deposition of the oxide film, the active region was encapsulated by the insulating epoxy resin (Easypoxy K-22 Conap), followed by the attachment of an O-ring seal (VT-76255, VITON). Finally, the active area of the entire device was covered with a removable glass window on the top. Electrical contacts of individual Cu electrodes were revealed by the selective mask and the final device was completed, as described schematically in figure 1. Inset (*a*) of figure 1 shows the Au particles inside ACF captured by an OM microscope. The back of the packaging of the device for the electrical measurement is also shown in inset (*b*) of figure 1.

2.2. Hydrogen sulfide detection experiments

The source of H_2S gas was fabricated using 10 g of thioacetamide (CH_3CSNH_2) powders (Tokyo Chemical Inc. Japan) dissolved in hot water (100 °C, 100 ml) for 3 min. Before the measurement commenced, all gas flows were routinely calibrated by $QRAE^+$ instrument (PGM 2000, 1 ppm of the resolution, detection range was from 0 to 100 ppm, RAE Inc.). Gas delivered to the sensor was simply provided by GASTIGHT #1010 syringe filled with the target gas, which was mixed with a carrier gas (N_2) injected in the reaction area. At high operational temperature, N_2 gas was heated to the target temperature and then injected into the reaction area with a flow rate of 28 ml min^{-1}. The inlet and outlet parts were implemented by utilizing three syringe needles (26 gauge and $\frac{1}{2}$ inch, BD-bioscience) piercing through the insulating epoxy resin. A syringe pump (Model KDS-100, KD Scientific) was employed to apply flow rates to achieve adjustable gas concentrations. A Keithley 237 source-measure unit (a ramping step of 2.5 V and a constant current of 1 nA) was connected to the solid-state device externally. After anode and cathode electrodes were arranged, the H_2S-modulated and differential-potential characteristics of the device were measured by sweeping the current–voltage measurement. A Keithley Programmable Electrometer (Model 617) was used to track the time-variant potentiometric outputs between the electrodes, as shown in figure 1. A GPIB (general purpose interface bus) interface and the LabView-based program were employed for recording the experimental results.

3. Results and discussion

Prior to applying the pressing force for the attachment of ACF and Cu-electrodes, the operation platform was heated to 185 °C for yielding the solid and good adhesion on the device surface. To seek for the optimal pressing strength used on ACF based on the obtained peak current, the cyclic voltammetry experiment (CV-50, from BAS Inc.) was

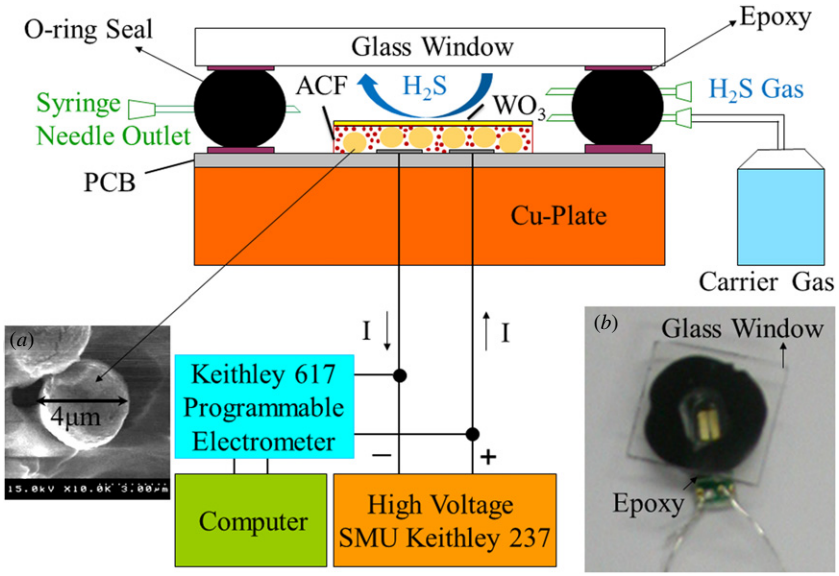

Figure 1. Schematic of the gas sensor proposed in our measurement system was connected to a current supplier and a programmable electrometer externally. The active region was encapsulated by the insulating epoxy resin (Easypoxy K-22 Conap) and an O-ring seal (VT-76255, VITON). The active area of the entire device was covered with a removable glass window on the top. Two Cu electrodes on the PCB were connected to positive (+) and negative (−) terminals of the power supplier (High Voltage SMU Keithley 237). A Keithley Programmable Electrometer (Model 617) was in shunt to the positive and negative terminals of the device. The target gas is injected with the mixture of a carrier gas and H_2S gas to achieve the adjustable gas concentrations in the reaction area. (Inset (*a*) displays the Au particles inside ACF shown by an OM microscope and the size of the gold (Au) particles is about 4 μm. Inset (*b*) shows the back of the packaging of the device for experiment.)

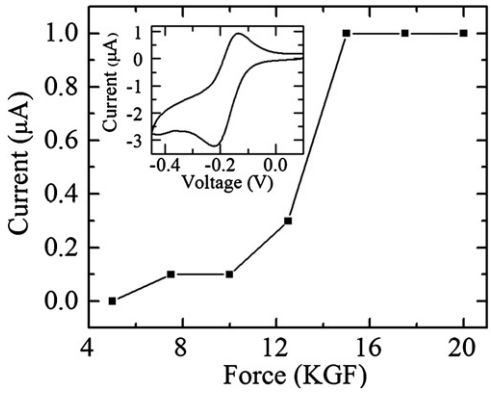

Figure 2. At 185 °C, the correlation plot of post-pressing force versus peak conduction current of the device was obtained according to a cyclic voltammetry measurement (CV-50, from BAS Inc.) in the solution (500 ml) of 1 mM $Ru(NH_3)_6Cl_3$ + 0.1 M $KClO_4$ mixture by applying the 50 mV s^{-1} scanning rate and −0.4 V to +0.4 V operation range. (Inset: cyclic voltammetry curve was measured based upon the optimal strength of the post-suppression (15 kgf) for 15 s.)

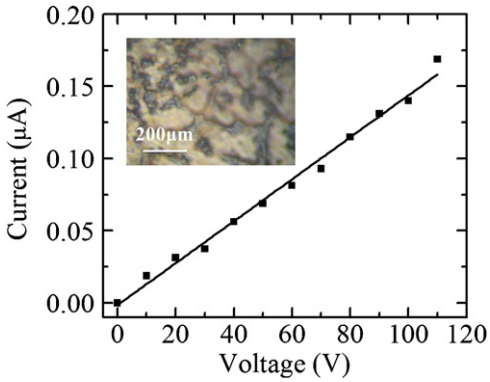

Figure 3. The correlation plot of the current–voltage characteristic was obtained by applying voltage from 0 to 110 V externally. (Inset picture is an OM micrograph of the WO_3 film coated on ACF/Cu electrode.)

utilized to determine the process condition by applying the 50 mV s^{-1} of scanning rate and −0.4 V to +0.4 V of operation range. Shown in figure 2, the optimal force of 15 kgf applied by a hot press machine (8122B, Hung-Ta Inc.) is recorded according to the correlation plot of the peak conduction current versus the pressing force. Firstly, ACF/Cu-electrode was processed to show the conductivity in the solution (500 ml) of 1 mM $Ru(NH_3)_6Cl_3$ + 0.1 M $KClO_4$ mixture with N_2 purge before the measurement started. As can be seen in figure 2, the typical oxidation and reduction characteristics of the ACF/Cu-electrode elucidate that the conductive interconnection is eligible to be a good electrode in this work.

The thickness of WO_3 deposition plays a crucial role in the impedance measurement across the electrodes during sensing of H_2S gas. After 4 h deposition of WO_3 film (3000 Å), the device reaches the optimal sensitivity (17.2) and declines out of the optimal thickness range. In figure 3, the current–voltage characteristic shows the high impedance performance by applying 0 to 110 V with a Keithley 237 source measurement unit. A microscopic micrograph of the WO_3 film coated on

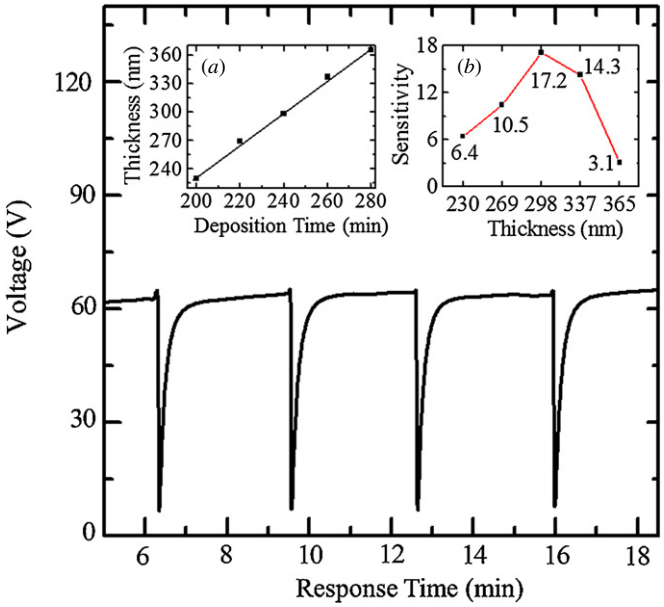

Figure 4. Repeatability performance measured from the typical response–recovery characteristic based on a fixed gas concentration (5 ppm) and volume (2 ml) applied at room temperature. The rising and recovery times are defined as 20% to 80% of the rising edge and falling edge in the transient response. The maximum ramp-up time is less than 10 s and the recovery time is within 25 s. (Inset pictures are (*a*) correlation plot of WO_3 film deposition time versus film thickness, and (*b*) optimal thickness of WO_3 film deposition according to the measured sensitivity.)

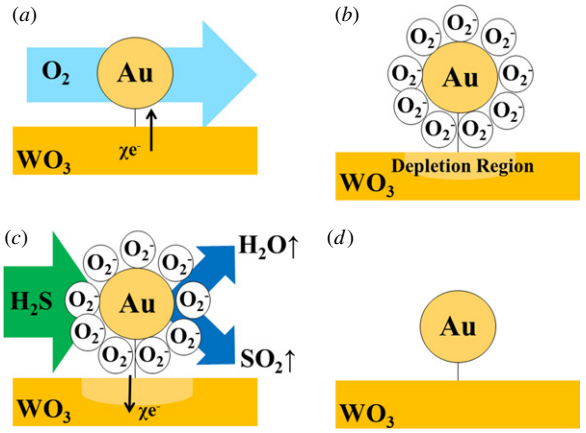

Figure 5. Reaction schemes for H_2S gas reduction reaction over supported Au catalysts: (*a*) physical adsorption is formed as oxygen molecules are approaching the Au-catalyzed interface, possibly on O_2 vacancies. Atmospheric oxygen adsorbs electrons from the conduction band of the sensing metal oxide and occurs on the surface in the form of O_2^- [28]. (*b*) Oxygen adsorption reaction occurs prior to H_2S-sensing, creating a thin electron-depleted layer at the surface of Au-incorporated WO_3 oxide. (*c*) As H_2S molecules are adsorbed, electrons are released into the conduction band according to reaction (a.2). (*d*) Further, the oxygen vacancies can easily be reoxidized upon exposure to fresh air, thereby assuring complete recovery [26].

ACF film shows that the grain sizes were about 100 to 250 μm as shown in the inset of figure 3.

In figure 4, the sensitivity is proportional to the WO_3 film thickness in the deficiency region of WO_3 thickness. After Au particles inside ACF film are submerged gradually by WO_3 film deposition, the efficiency of catalyzed conductivity will be attenuated and the detection will be terminated. It is noted that our sputtering system performs with a linear characteristic according to the correlation plot of time versus film thickness, as shown in the inset of figure 4. All experiments were processed in an atmospheric pressure and at a relative humidity of 50–55%. These measured results have repeatable characteristics and rapid transient responses based upon periodic waveforms by supplying 5 ppm and 2 ml of H_2S gas at room temperature.

According to the double Schottky barrier model [22–25], O_2 molecules adsorbed on grain boundaries on the bulk surface will extract electrons in the conduction band and trap electrons in the form of reduced O_2^- ions at the surface. Considering the n-type WO_3-based sensor we proposed, the resistance will decrease in the presence of reducing species and increase in the presence of oxidizing species. A space-charge region will be generated when oxygen adsorption occurs prior to H_2S-sensing. The work function at the interface of the target gas and Au-incorporated WO_3 surface will be decreased [26]. In the experiments, O_2 adsorption has been believed to occur mainly at the Au-catalyzed interface, possibly on O_2 vacancies [13], which should be present on semiconductor materials, especially in the proximity of the Au particles as a consequence of the Schottky junction at the metal–semiconductor interface [27], as depicted schematically in figure 5(*a*)–(*d*). As H_2S is adsorbed, electrons are released into the conduction band. Water vapor and SO_2 gas will be produced as the byproduct after each reaction. Therefore, the available sites on the sensor surface will be generated for undergoing next chemical reactions according to reactions (a.1) and (a.2) at room temperature. The resistance of the metal-oxide will decrease when it comes into contact with H_2S gas. It is expected that the resistance change upon exposure to H_2S gas is mainly due to the resistance change of the Au-incorporated WO_3:

$$O_2(g) + e^- \leftarrow\rightarrow O_2^-(ads) \qquad (a.1)$$

$$2H_2S(g) + 3O_2^-(ads) \leftarrow\rightarrow 2H_2O + 2SO_2 + 3e^-, \qquad (a.2)$$

where (g) and (ads) denote gas phase and adsorbed species, respectively. Reaction (a.1) takes place prior to gas sensing and creates a thin electron-depleted layer at the surfaces of the WO_3 grains. As H_2S is adsorbed, electrons are released into the conduction band based on reaction (a.2), resulting in higher conductivity thereby increasing the sensitivity [25].

The gas sensitivity (S) is defined as the ratio R_{air}/R_{gas}, where R_{air} and R_{gas} stand for the resistances measured in air and in a test gas, respectively. Under the constant concentration (10 ppm) and current (1 nA) supplied, the sensitivity is intrinsically proportional to H_2S gas volume delivered externally. Based on the response–recovery characteristic, the fitting slope characterized good linearity from 0.5 to 2.5 ml of the H_2S gas injected, as shown in figure 6. At room temperature, the sensitivity is as high as 6.1 and 51.6 by applying 0.5 and 2.5 ml H_2S gas, respectively. Also, the sensitivity proportional to the concentration variation is as

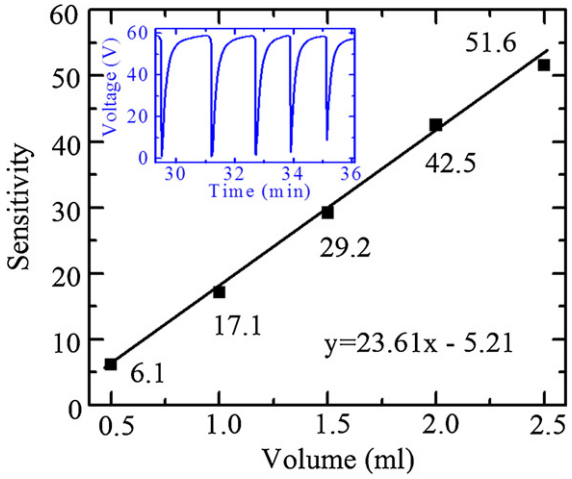

Figure 6. Sensitivity as a function of H_2S gas volume based on the response–recovery characteristic under a fixed gas concentration (10 ppm) by applying different gas volumes (0.5 ml to 2.5 ml) at room temperature. (Inset: dynamic response of voltage variation with different H_2S gas volumes.)

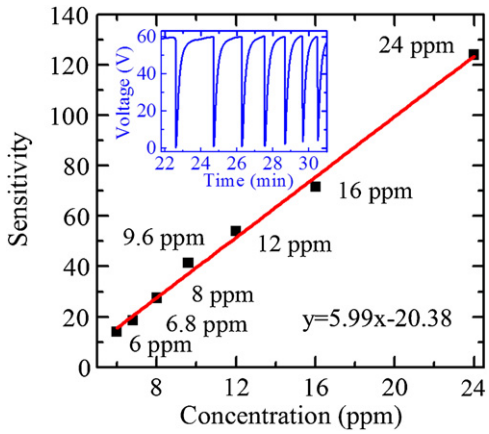

Figure 7. Sensitivity as a function of H_2S gas concentration based on the response–recovery characteristic under a fixed gas volume (2 ml) by applying different concentrations (6–24 ppm) at room temperature. (Inset: dynamic response of voltage variation with different H_2S gas concentrations.)

Table 1. Comparison of the sensor with/without ACF impregnated with the same volume and concentration of H_2S gas by applying 2 ml of volume and 24 ppm of concentration at room temperature.

Parameter	With ACF	Without ACF
Volume (ml)	2	2
Concentration (ppm)	24	24
Sensitivity ($S = R_{air}/R_{gas}$)	122.7	2.8

high as 122.7 by applying 24 ppm of H_2S concentration at room temperature. The sensitivity can be calculated according to the exact volume injected, as illustrated in figure 7.

Comparing with the counterpart without ACF film, significant improvement has been observed with 24 ppm of H_2S gas concentration using the straightforward structure we proposed, as summarized in table 1. Obviously, Au particles inside ACF film will trigger the catalysis and improve the sensitivity significantly. Even in the low-level concentration

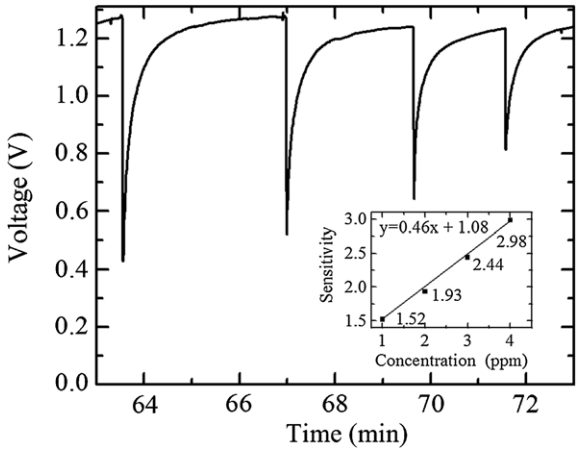

Figure 8. Response–recovery characteristic of voltage variation versus time with different H_2S gas concentrations (2 ml) by applying different concentrations (1–4 ppm) at room temperature. (Inset: extra-small H_2S gas concentration with a fixed volume and measured sensitivity from the response–recovery characteristic.)

Table 2. Comparison of the sensitivity to different types of gas including H_2S, H_2, CH_4, and CO_2 based on different gas concentrations and the same volume (2 ml).

Gas type	H_2S	H_2	CH_4	CO_2
Concentration (ppm)	10	10^3	10^3	10^3
Sensitivity ($S = R_{air}/R_{gas}$)	41	1	1	1

of H_2S gas injected, the device performs with good linearity and repeatable characteristic, as shown in figure 8, and the sensitivity is 1.52 with 1 ppm H_2S gas. In the low concentration detection as shown in figure 8, it depicts a good linear characteristic of the sensitivity versus concentration correlation with a high R^2 value (0.999), and it is believed that the sensitivity resolution can be as small as 0.2 ppm. All the measurement results perform rapid responses for the detection and short recovery time for settling down. The rising and recovery times are defined as 20% to 80% of the rising edge and falling edge in the transient response. The maximum ramp-up time is 10 s and the recovery time is less than 35 s. The time constant of each response is caused by the combinations of equilibrium capacitance and resistance generated from the region of depletion. During room-temperature sensing, the long response time can be explained based on the slow reaction rate of H_2S with adsorbed oxygen ions (reaction (a.2)). The long recovery time is due to incomplete desorption of the adsorbed reaction products and H_2S gas after finishing the H_2S exposure [25]. The sensitivity can be up to 41 with less than 10 ppm of H_2S gas injected at room temperature. As summarized in table 2, with 10 ppm of the H_2S gas concentration and 1000 ppm of other gases (H_2, CH_4, and CO_2) with the same volume (2 ml) applied individually, the performance distinguishes the gas species clearly and exhibits the excellent selectivity.

Table 3 tabulates a comparison of this work with respect to other Au-dopant driven WO_3 solid-state sensors. The figure of merit for the sensitivity performance is characterized

Table 3. Comparison of the various types of sensors with different fabrication methods, applied gas concentrations (0.1–10 ppm) and different operating temperatures.

Production method	Concentration (ppm)	Operating temperature (°C)	Sensitivity ($S = R_{air}/R_{gas}$)	Reference
WO_3	1	28	1.52	This work
WO_3	10	28	41	This work
nano-WO_3	5	327	10	[25]
nano-WO_3	10	327	20	[25]
nano-WO_3	1	28	1.5	[13]
nano-WO_3	10	220	10	[13]
nano-WO_3	0.1	110	4.1	[9]
nano-WO_3	0.1	200	11.14	[9]

in terms of production method, gas concentration and operation temperature. The sensitivity profile of the Au-doped WO_3 gas sensor was demonstrated as a function of operating temperature up to 220 °C [13] and increases when the operation temperature goes higher. The sensitivity is 1.5, under 1 ppm of H_2S gas concentration at room temperature, and 10, under 10 ppm at 220 °C. Stankova *et al* demonstrated that the sensitivity is 4.1 and 11.14 at 110 °C and 200 °C, respectively, under 1 ppm of H_2S gas concentration [9]. The Hoel group performed the linear characteristic of the sensitivity versus H_2S concentration correlation from 5 to 35 ppm at high temperature [25]. Operating at room temperature, our sensor using the hybrid integration process exhibits compatible performance with sensors fabricated by other methods.

4. Conclusions

In summary, different from conventional fabrication methods, we have developed a solid-state H_2S gas sensor using a new hybrid approach comprising ACF/Cu electrodes, followed by a WO_3-sputtered film deposition. With the appropriate strength of the pre- and post-suppression applied for the attachment of ACF and Cu-electrodes, the electrical conductivity of our device has been examined as a linear characteristic of H_2S gas volume versus the supplied concentration. The work function at the interface of the target gas and on Au-incorporated WO_3 surface will be decreased. Au dopant-like particles in ACF will produce a lower barrier between the bands of electrons, and thus improve the conductivity significantly. The proposed sensor exhibits a high sensitivity to H_2S gas even in the low-level injection and the sensitivity can be up to 41 with 10 ppm concentration at room temperature. Additionally, the performance distinguishes the gas species clearly and exhibits good selectivity by applying H_2, CH_4 and CO_2 gas individually in the experiments. Our method offers a number of merits, including high sensitivity to the reference gas, lead-free bonding connection, low-temperature operation, higher throughput and the reduction of fabrication time.

Acknowledgments

LMK would like to acknowledge the scholarship and support from Chung-Shan Institute of Science and Technology (CSIST), Taoyuan, Taiwan and National Defense Industrial Development Foundation (NDIDF), Taipei, Taiwan. The authors express their thanks to Ms Holli Kinstle, Language Teaching and Research Center of National Chiao Tung University, Hsinchu, Taiwan, for her support in writing the manuscript.

References

[1] Grunert K G 2005 Food quality and safety: consumer perception and demand *Eur. Rev. Agric. Econ.* **32** 369–91
[2] Muehling A J 1970 Gases and odors from stored swine waste *J. Anim. Sci.* **30** 526–30
[3] Guidotti T L 2010 Hydrogen sulfide: advances in understanding human toxicity *Int. J. Toxicol.* **29** 569–81
[4] Bhambhani Y, Burnham R, Snydmiller G and MacLean I 1997 Effects of 10-ppm hydrogen sulfide inhalation in exercising men and women cardiovascular, metabolic, and biochemical responses *J. Occup. Environ. Med.* **39** 122–9
[5] Miura N, Yan Y, Lu G Y and Yamazoe N 1996 Sensing characteristics and mechanism of hydrogen sulfide sensor using stabilized zirconia and oxide sensing electrode *Sensors Actuators* B **34** 367–71
[6] Tamaki J, Shimanoe K, Yamada Y, Yamamoto Y, Miura N and Yamazoe N 1998 Dilute hydrogen sulfide sensing properties of CuO-SnO_2 thin film prepared by low-pressure evaporation method *Sensors Actuators* B **49** 121–5
[7] Hoel A, Ederth J, Kopniczky J, Heszler P, Kish L B, Ollson E and Granqvist C G 2002 Conduction invasion noise in nanoparticles WO_3/Au thin-film devices for gas sensing application *Smart Mater. Struct.* **11** 640–4
[8] Solis J L, Suakko S, Kish L B, Granqvist C G and Lantto V 2001 Nanocrystalline tungsten oxide thick-films with high sensitivity to H_2S at room temperature *Sensors Actuators* B **77** 316–21
[9] Stankova M, Vilanova X, Llobet E, Calderer J, Vinaixa M, Gracia I, Cane C and Correig X 2006 On-line monitoring of CO_2 quality using doped WO_3 thin film sensors *Thin Solid Films* **500** 302–8
[10] Galipeau J D, Falconer R S, Vetelino J F, Caron J J, Wittman E L, Schweyer M G and Andle J C 1995 Theory, design and operation of a surface acoustic wave hydrogen sulfide microsensor *Sensors Actuators* B **24** 49–53
[11] Ippolito S J, Kandasamy S, Kalantar-Zadeh K, Wlodarski W and Holland A 2006 Comparison between conductometric and layered surface acoustic wave hydrogen gas sensors *Smart Mater. Struct.* **15** 131–6
[12] Lin H M, Hsu C M, Yang H Y and Lee P W 1994 Nanocrystalline WO_3-based H_2S sensors *Sensors Actuators* B **22** 63–8
[13] Tao W H and Tsai C H 2002 H_2S sensing properties of noble metal doped WO_3 thin film sensor fabricated by micromachining *Sensors Actuators* B **81** 237–47
[14] Xu Z, Vetelino J F, Lec R and Parker D C 1990 Electrical properties of tungsten trioxide films *J. Vac. Sci. Technol.* A **8** 3634–8
[15] Atsumi K, Kashima N and Maehara Y 1988 High-accuracy inner lead bonding technique *Toshiba Rev.* **43** 833
[16] Gilleo K 1989 Direct chip interconnect using polymer bonding technology *IEEE Proc. Electron. Connection Conf. (Houston, TX, May)* pp 37–44
[17] Chang S M, Jou J H, Hsieh A, Chen T H, Chang C Y and Wang Y H 2001 Characteristic study of anisotropic conductive film for chip-on-film packaging *Microelectro. Reliab.* **41** 2001–9
[18] Ishibashi K and Kimura J 1996 A new anisotropic conductive film with arrayed conductive particles *IEEE Trans. Compon. Packag. Manuf. Technol.* B **19** 752–7

[19] Pai R and Walsh K 2005 The viability of anisotropic conductive film as a flip chip interconnect technology for MEMS devices *J. Micromech. Microeng.* **15** 1131–9
[20] Chao S 1998 Electrical characteristics of CO_2-sensitive diode based on WO_3 and IrO_2 for microsensor applications *Japan. J. Appl. Phys.* **37** 245–7
[21] Kuo L M, Chen K N, Chuang Y L and Chao S 2013 A flexible pH-sensing structure using WO_3/IrO_2 junction with Al_2O_3 encapsulation layer *ECS Solid State Lett.* **2** 28–30
[22] Madou M and Morrison S R 1989 *Chemical Sensing with Solid State Devices* (Boston, MA: Academic)
[23] Ihokura K and Watson J 1994 *The Stannic Oxide Gas Sensor: Principles and Applications* (Tokyo: CRC Press)
[24] Frank M E, Koplin T J and Simon U 2006 Metal and metal oxide nanoparticles in chemiresistors: Does the nanoscale matter? *Small* **2** 36–50
[25] Reyes L F, Hoel A, Saukko S, Heszler P, Lantto V and Granqvist C G 2006 Gas sensor response of pure and activated WO_3 nanoparticle films made by advanced gas reactive gas deposition *Sensors Actuators* B **117** 128–34
[26] Datta N, Ramgir N, Kaur M, Roy M, Bhatt R, Kailasaganapathi S, Debnath A K, Aswal D K and Gupta S K 2012 Vacuum deposited WO_3 thin films based sub-ppm H_2S sensor *J. Mater. Chem. Phys.* **134** 851–57
[27] Schubert M M, Hackenberg S, Veen V A C, Muhler M, Plzak V and Behm R J 2001 CO oxidation over supported gold catalysts—'Inert' and 'Active' support materials and their role for the oxygen supply during reaction *J. Catal.* **197** 113–22
[28] Rout C S, Hegde M and Rao C N R 2008 H_2S sensors based on tungsten oxide nanostructures *Sensors Actuators* B **128** 488–93